# ARPES Spectra of the Hubbard model

Th. A. Maier,[1] Th. Pruschke,[2] and M. Jarrell[1]

[1] *Department of Physics,University of Cincinnati, Cincinnati OH 45221, USA*
[2] *Center for electronic correlations and magnetism, Theoretical Physics III, Institute for Physics, University of Augsburg, 86135 Augsburg, Germany*

We discuss spectra calculated for the 2D Hubbard model in the intermediate coupling regime with the dynamical cluster approximation, which is a non-perturbative approach. We find a crossover from a normal Fermi liquid with a Fermi surface closed around the Brillouin zone center at large doping to a non-Fermi liquid for small doping. The crossover is signalled by a splitting of the Fermi surface around the $X$ point of the $2D$ Brillouin zone, which eventually leads to a hole-like Fermi surface closed around the point $M = (\pi, \pi)$. The topology of the Fermi surface at low doping indicates a violation of Luttinger's theorem. We discuss different ways of presenting the spectral data to extract information about the Fermi surface. A comparison to recent experiments will be presented.

## Introduction

The rich phenomenology of high-$T_c$ superconductors[1] has stimulated strong experimental and theoretical interest in the field of strongly correlated electron systems. Apart from the anomalously high transition temperatures, these compounds are also of interest due to their unusual normal state properties. Most of these anomalous properties are found in spectra and transport quantities, i.e. are intimately linked to the dynamics of the electronic degrees of freedom. Thus, much of the experimental and theoretical effort has concentrated on the development of an understanding of the single-particle dynamics. Among the fundamental and controversial questions are whether the cuprates can be described as a Fermi liquid or not and what shape and volume a possible Fermi surface will have.

In this connection, one of the most informative experimental probes of the cuprates has become the Angle-Resolved Photoemission Spectroscopy(ARPES). The development in this field, again largely stimulated by the interest in the physics of high-$T_c$, has led to a tremendous increase of the angular and energy resolution[2,3]. ARPES is now able to access the low-energy behavior of single-particle spectra and especially the shape and topology of the cuprate Fermi surface. This has lead to the discovery of the shadow bands[1,4] and the pseudo-gap formation in the underdoped cuprates[1]. Recently, the single-particle self energy was extracted from the ARPES data, showing extremely interesting behavior especially close to $(\pi/2, \pi/2)$ on the Fermi surface[5].

A large number of the more recent ARPES experiments have concentrated on Fermi surface mapping. Some of these experiments seem to indicate that, at least for LSCO, the Fermi surface switches from being hole-like, centered at $M = (\pi, \pi)$, for low doping to being electron-like, centered at the zone center $\Gamma = (0, 0)$ for high doping with a volume consistent with the doping level[3,6,7]. In other results, particularly for bilayer compounds like YBCO or Bi2212[3,8], the Fermi surface seems to remain hole-like independent of the doping level. Especially for those latter compounds, further complications in the experiments arise from superstructures due to umklapp scattering and the possibility of bilayer splittings in YBCO and Bi2212[3,9]. Furthermore, in the underdoped regime one can observe additional changes in the Fermi surface topology that are frequently brought in connection with the possibility of stripe formation in LSCO[3].

The presence of a large Fermi surface has been taken as a validation of Luttinger's theorem; however, other results find that the Fermi surface volume, at least in the underdoped regime, is too small[8], which would point towards a violation of Luttinger's theorem. Furthermore, recent experiments seem to indicate that the low doping Fermi surface near $X = (\pi, 0)$ actually bifurcates into two parts, one electron-like and one hole-like[10]. This splitting has been interpreted in terms of strong interlayer coupling[9], but could equally well result from shadow Fermi surface formation due to coupling of the electrons to strong antiferromagnetic fluctuations around the $X$ points[8].

Thus, a consistent experimental picture concerning both shape and volume of the Fermi surface is at present not available and a theoretical investigation of the generic features to be expected based on a model calculation is necessary.

Early in the theoretical investigation of the high-$T_c$ cuprates it was realized that the 2D Hubbard model

$$H = \sum_{i,j,\sigma} t_{ij} c^\dagger_{i\sigma} c_{j\sigma} + \frac{U}{2} \sum_{i\sigma} c^\dagger_{i\sigma} c_{i\sigma} c^\dagger_{i\bar{\sigma}} c_{i\bar{\sigma}} \qquad (1)$$

in the intermediate coupling regime, or closely related models like the $t$-$J$ model probably capture the essential physics[11]. In the wake of this conjecture, a huge effort has been directed to the study of these models[12]. There is now a general consensus that the appropriate parameter regime for the cuprates is the intermediate coupling regime where the Coulomb parameter $U$ is roughly equal to the bandwidth. However, this is the most complicated regime of the model since both weak and strong coupling perturbative approaches fail. Exact diagonal-

ization of small clusters[12] suffers from strong finite-size effects, often ruling out the reliable extraction of low-energy dynamics. Conventional Quantum Monte Carlo for finite sized systems suffers from a severe minus sign problem in this parameter regime. The resulting data is of insufficient quality to allow for reliable calculations of dynamic quantities at low enough temperatures. High-temperature series has provided some of the most informative results for the Fermi surface topology, but it does not yield spectra, and, so far, only results for the t-J model are available[13].

Thus, also from a theoretical point of view, the question of whether a Fermi surface does actually exist and what its topology is still is a matter of debate. In that connection it is of special interest that some experiments indicate a violation of Luttinger's theorem; if true, any theory, such as FLEX[14], based on a weak-coupling expansion around the non-interacting limit would be inadequate.

Thus a treatment within a non-perturbative scheme clearly is desirable. In this paper we therefore use the recently developed dynamical cluster approximation (DCA)[15,16,17,18,19] to study the low-energy behavior of the $2D$ Hubbard model in the intermediate coupling regime with nearest-neighbor hopping $t$ and on-site correlation $U$ equal to the band width $W$. The DCA systematically incorporates non-local corrections to local approximations like the dynamical mean field, by mapping the lattice onto a self-consistently embedded cluster. We solve the cluster problem using a combination of quantum Monte Carlo (QMC) and the maximum entropy method to obtain dynamics. This technique produces results in the thermodynamic limit and has a mild minus-sign problem[19].

The paper is organized as follows. The next section contains a brief introduction to the DCA. The numerical results will be presented in the third section followed by a discussion and summary.

## Formalism

A detailed discussion of the DCA formalism was already given in previous publications[15,16,17,18,19]. The main assumption underlying the DCA is that the single-particle self-energy $\Sigma(\vec{k}, z)$ is a slowly varying function of the momentum $\vec{k}$ and can be approximated by a constant within each of a set of cells centered at a corresponding set of momenta $\vec{K}$ in the first Brillouin zone[15]. The single-particle lattice Green functions are then coarse-grained or averaged within these cells, and used to calculate the lattice self energy and other irreducible quantities. Within this approximation, one can set up a self-consistency cycle similar to the one in the dynamical mean-field theory (DMFT)[20]. However, in contrast to the DMFT, where only local correlations are taken into account, the DCA includes non-local dynamical correlations. The length scales of these non-local correlations can be varied systematically from short ranged to long ranged by increasing the number of coarse-graining cells. The DCA collapses to the DMFT if one represents the Brillouin zone by one cell only, thus setting the characteristic length scale to zero.

By construction, the DCA preserves the translational and point group symmetry of the lattice. Comparisons to other extensions of the DMFT developed during the past years[21,22] either show that these are identical to the DCA or converge more slowly as function of cluster size[23].

For the impurity problem of the DMFT a large set of reliable numerical techniques has been developed over the past ten years[20,24,25]. We have employed Quantum Monte Carlo (QMC) and the Non-Crossing Approximation (NCA)[16] as non-perturbative (in $U$) methods to solve the cluster problem of the DCA. For cluster sizes larger than $N_c = 4$ however, only the QMC technique is presently available for the DCA. The cluster problem is solved using the Hirsch-Fye impurity algorithm[26] modified to simulate an embedded cluster[19]. Note that this problem is computationally much more difficult than that encountered in either the DMFA or in finite-sized simulations, since the block diagonal structure in space-time occurring in conventional finite-system simulations is not present here. This increase in computation time is, however, partially compensated by a rather mild minus-sign problem, even for comparatively large values of $U$ and small temperatures[19]. From the QMC data, the spectra are obtained by analytic continuation with the maximum entropy method[27]. Finally, the self energy is interpolated on to the full Brillouin zone using Akima splines, which is a sensible step as long as the assumption of a slow variation in **k**-space is valid. Note that it is very important to interpolate irreducible quantities like the self energy and *not* for example the cluster Green function itself.

## Results

For a proper description of the $CuO_2$ planes of the high-$T_c$ cuprates within the Hubbard model (1) it is generally accepted that the tight-binding dispersion has the form

$$t_{\vec{k}} = -2t\left(\cos(k_x) + \cos(k_y)\right) - 4t' \cos(k_x)\cos(k_y) \quad (2)$$

with a nearest neighbor hopping amplitude $t > 0$ and a next-nearest neighbor hopping amplitude $t'$, which in principle can have any sign. From bandstructure calculations and the general form of the measured Fermi surface, especially in the overdoped regime, conventionally a negative $t'$ is inferred[28]. Such a negative $t'$ would naturally lead to a Fermi surface closed around the Brillouin zone corner $M$. The interesting question, however, is whether the Fermi surface closed around the $M$ point observed experimentally in the low-doping region is a mere

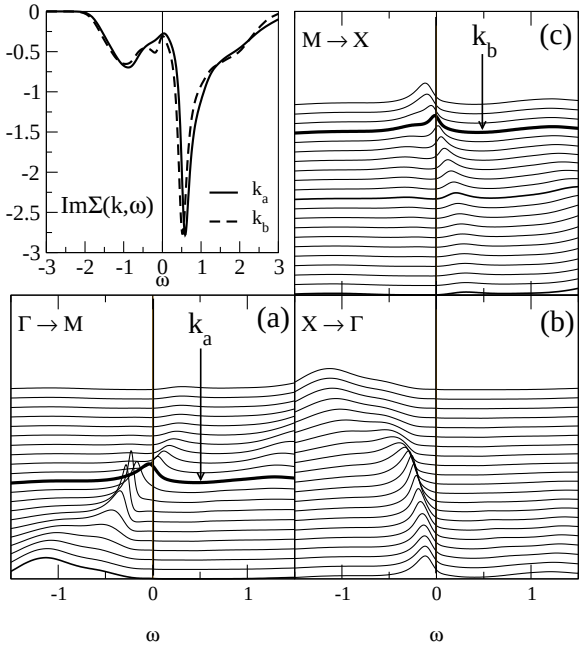


FIG. 1: (a)–(c) The single-particle spectrum $A(\mathbf{k},\omega)$ for $U = 2$eV, $T = \frac{1}{30}$eV, $\delta = 0.05$, $t_\perp = 0$ and $N_c = 16$ along certain high symmetry directions (spectra for different $\mathbf{k}$ are shifted along the y-axis). The colored lines in Figs. (a) and (c) indicate the spectra which cross the Fermi energy with a peak closest to $\omega = 0$. In (b), no such peak is found which crosses the Fermi energy. (d) the imaginary part of the self energy versus frequency at the Fermi surface crossing found in (a) and (c).

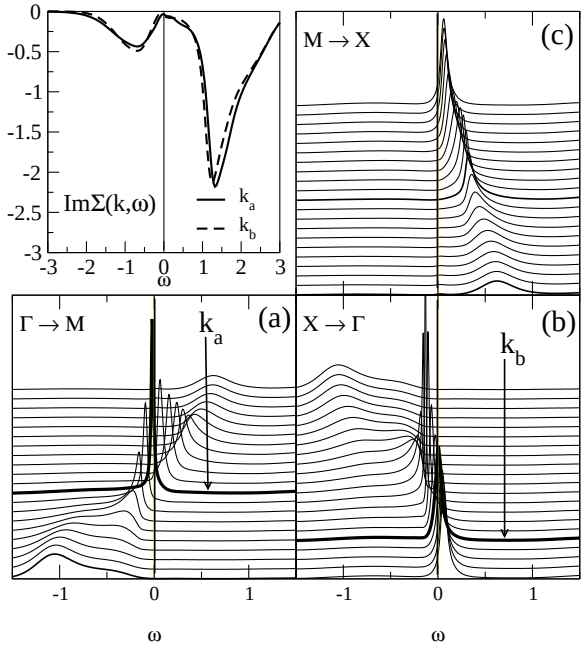


FIG. 2: (a)–(c) The single-particle spectrum $A(\mathbf{k},\omega)$ $\delta = 0.20$ along certain high symmetry directions. Other parameters as in Fig. 1. The colored lines in Figs. (a) and (b) indicate the spectra which cross the Fermi energy with a peak closest to $\omega = 0$. In (c), no such peak is found which crosses the Fermi energy. (d) the imaginary part of the self energy versus frequency at the Fermi surface crossing found in (a) and (b).

bandstructure effect or induced by correlations. Weak coupling treatments of the $2D$ Hubbard model indicate that such a change of the shape, but not the volume, of the Fermi surface due to the interactions is indeed possible[14,29]. Thus, to obtain insight into the effects of correlations on the structure of the Fermi surface and distinguish them from pure bandstructure effects, we concentrate on the case $t' = 0$ in this paper.

In the following we set $t = 1/4$eV in accordance with typical values extracted from the experiments and bandstructure and choose $U = W = 2$eV. This value of $U$ is sufficiently large that for $N_c \geq 4$ a Mott gap is present in the half-filled model[30]. We performed our simulations at a range of temperatures, but will present results for $T = 0.033$eV only, which is roughly room temperature. A pseudogap due to short-ranged spin correlations is also present in the weakly doped model for slightly lower temperatures[19].

The single-particle spectra for certain high symmetry directions are plotted in Figs. 1 and 2 for $n = 0.95$ and $n = 0.80$, respectively. We use the standard convention to identify the high symmetry points in the zone, $\Gamma = (0,0)$, $M = (\pi,\pi)$ and $X = (\pi,0)$. For $n = 0.95$ the peak in the spectrum crosses the Fermi energy along the $\Gamma \to M$ and $M \to X$ directions, while for $n = 0.80$ the second crossing appears along $X \to \Gamma$. The imaginary part of the self energy at these crossing points is plotted versus frequency in panel (d) of Figs. 1 and 2.

One very interesting feature of the spectra at low doping, Fig. 1, is that the peak near $(\pi/2,\pi/2)$ broadens dramatically before crossing the Fermi energy. Near $X$, on the other hand, one does not observe any dramatic change in the spectrum when crossing the Fermi energy. This indicates that near $(\pi/2,\pi/2)$ hole-like quasiparticle (QP) excitations with $k < k_F$ appear to have longer lifetimes than electronic excitations with $k > k_F$. This asymmetry between particles and holes near the Fermi surface is a strong indication of non-Fermi liquid (NFL) behavior, at least along the $\Gamma$-$M$ direction. Note that this is at least qualitatively in agreement with experimental ARPES spectra[3,31]. Although these experiments on LSCO had to be performed below $T_c$ in the underdoped sample[31], the authors infer from the general behavior of the spectra, that a peak crossing the Fermi energy can be found along $M \to X$, while a rather broad structure is seen along $\Gamma \to M$ around $(\pi/2,\pi/2)$. It would clearly be interesting to have experimental ARPES data above $T_c$ available for a more founded comparison.

It is also quite instructive to look at the imaginary part of the self-energy at the $\mathbf{k}$-points where the peak in the spectrum crosses the Fermi energy (Fig. 1(d)). In particular at the crossing point $\mathbf{k}_b$ close to $(\pi,0)$, $\Im m\Sigma(\mathbf{k}_b,\omega)$ shows a striking asymmetry in the low-frequency regime as compared to $\Im m\Sigma(\mathbf{k}_a,\omega)$, where $\mathbf{k}_a$ is the crossing

point close to $(\pi, 0)$. In fact, $\Im m\Sigma(\mathbf{k}_b, \omega)$ starts to develop an additional feature which eventually leads to the formation of a pseudo gap in the spectra along the $M \to X$ direction[19]. In addition, one observes a rather large residual scattering rate for both momenta $\vec{k}_a$ and $\vec{k}_b$. This can either be taken as further evidence for NFL behavior or as signal for the occurrence of a new very small low-energy scale[32]. Obviously, we cannot decide this question on the basis of the present data, but would have to look at much lower temperatures. Unfortunately, this is not possible at present. Note that in the low-energy regime the self energy displays significant $k$-dependence. This clearly renders theories based on a local approximation like the DMFA inadequate at least for small doping.

At higher doping, Fig. 2, the peaks in the spectrum close to the Fermi energy are far sharper. Here it makes sense to speak of a conventional Fermi liquid and quasi particles again. As already mentioned, the Fermi energy crossings can be found along $\Gamma \to M$ and $X \to \Gamma$. Again, this is in qualitative accordance with ARPES experiments for strongly overdoped LSCO[3,31], although these experiments still find rather broad structures even in heavily overdoped samples. In addition, there is no evidence for particle-hole asymmetry in our data. Especially at $(\pi/2, \pi/2)$ the structure crossing the Fermi level appears to be rather symmetric with respect to the crossing point.

The imaginary part of the self energy, shown in Fig. 2(d), has a broad maximum at $\omega = 0$ with a very small residual scattering rate and changes little as $\mathbf{k}$ moves along the Fermi surface. This weak dependence on $\mathbf{k}$ is an indication that approximations like the DMFA should be accurate here, i.e. that there is little effect of non-local correlations. All indications are that for this doping regime standard Fermi-liquid behavior has returned.

More evidence for NFL behavior can be seen in the shape of the Fermi surface. Theoretically, the Fermi surface can be defined in two different ways. First, the gradient of the electronic distribution function, $|\nabla n(\mathbf{k})|$, has a maximum at the Fermi surface. From a computational point of view this quantity is very convenient, because it does not require the calculation of dynamical properties. However, especially for a comparison with experimental Fermi surface mappings based on ARPES experiments, the approach via $|\nabla n(\mathbf{k})|$ probably is not adequate, mainly due to the unknown influence of matrix elements in the experimental spectra[2].

An analysis of the Fermi surface for the $t$-$J$ model based on a study of $|\nabla n(\mathbf{k})|$ has been performed recently within a high-temperature expansion[13] and been considered as clear evidence for a violation of Luttinger's theorem and the possible formation of a non-Fermi liquid at small doping. Our results for that quantity are collected in Figs. 3 and 4, where $|\nabla n(\mathbf{k})|$ for the upper right quadrant of the first Brillouin zone is shown in a density plot for $n = 0.95$ and $n = 0.8$, respectively. Regions of large values of $|\nabla n(\mathbf{k})|$ are colored in blue and violet, regions of small values in red. For comparison the Fermi surface for the non-interacting system is included (black line). For small doping, Fig. 3, $|\nabla n(\mathbf{k})|$ gives a rather broad structure around $(\pi/2, \pi/2)$ rather following the noninteracting Fermi surface. It is especially hard to define a Fermi surface at all or extract a reliable estimate of the Fermi surface volume from these results. Note also the strong bifurcation around the $X$ points. We find that especially for small doping $|\nabla n(\mathbf{k})|$ generally predicts that the Fermi surface bifurcates near $X$, with parts of the Fermi surface along both $M \to X$ and $X \to \Gamma$. This is in striking contrast to the fact that the spectra in Fig. 1 do not show a crossing along the direction $X \to \Gamma$, only a peak coming close to the Fermi energy. Apparently, $|\nabla n(\mathbf{k})|$ is unable (at least at these temperatures) to distinguish between a peak in the spectrum crossing or just simply approaching the Fermi energy.

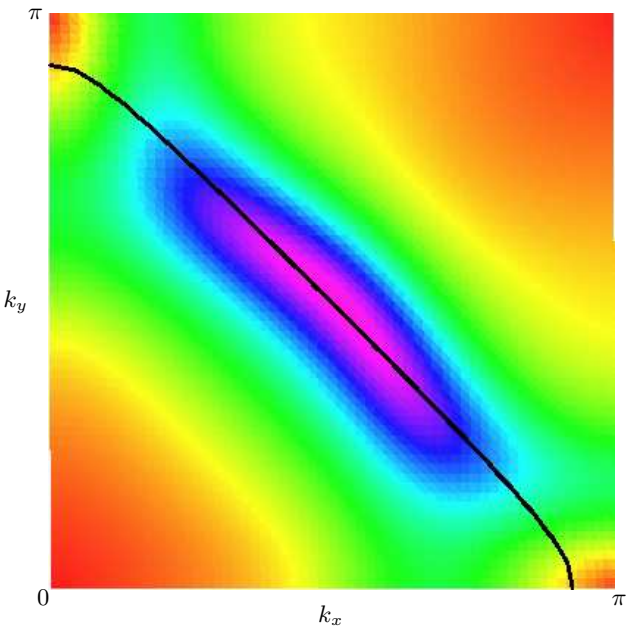


FIG. 3: Gradient of the distribution function $|\nabla n(\mathbf{k})|$ for $U = 2$eV, $T = \frac{1}{30}$eV, $\delta = 0.05$, $t_\perp = 0$ and $N_c = 16$. Shown is the upper right quadrant of the first BZ. The violet (red), represents regions of high (low) values. The blue and violet regions map out the Fermi surface. The non-interacting Fermi surface is shown by the black line. The interacting Fermi surface is rather hard to define. Note the strong bifurcation around the $X$ points.

In accordance with the spectra in Fig. 2, the plot of $|\nabla n(\vec{k})|$ for large doping in Fig. 4 shows a fairly well defined Fermi surface that coincides with the Fermi surface of the non-interacting system. Again, in contrast to the sharp peaks found in the spectra, $|\nabla n(\vec{k})|$ shows a substantial broadening, which in this case can however be explained by the conventional temperature broadening of Fermi's function.

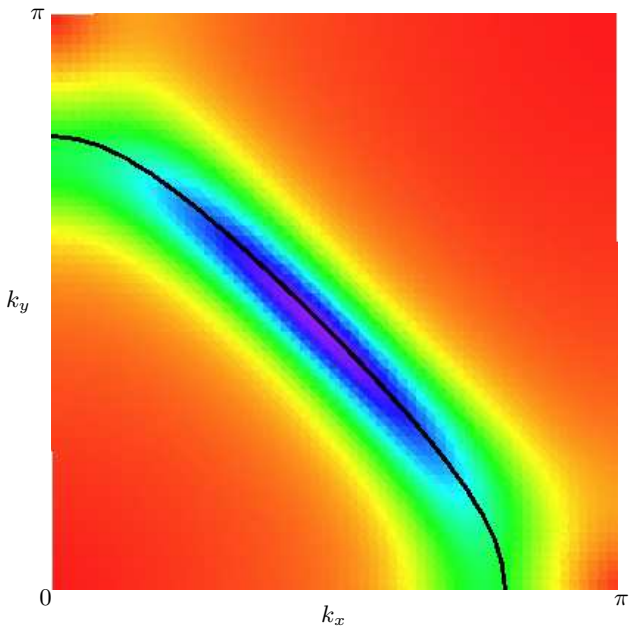


FIG. 4: $|\nabla n(\mathbf{k})|$ for $U = 2$eV, $T = \frac{1}{30}$eV, $\delta = 0.20$, $t_\perp = 0$ and $N_c = 16$. The color scheme is the same as in Fig. 3. The non-interacting and interacting Fermi surfaces coincide, in accord with Luttinger's theorem.

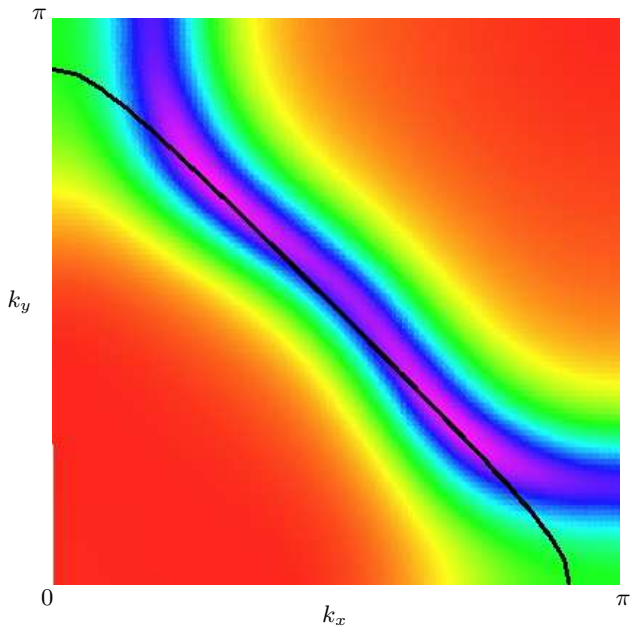


FIG. 5: Constant energy scans of $A(\mathbf{k}, \omega = 0)$ for $U = 2$eV, $T = \frac{1}{30}$eV, $\delta = 0.05$, $t_\perp = 0$ and $N_c = 16$ in the right upper quadrant of the first BZ. The violet (red), represents regions of high (low) electronic density. The blue and violet regions map out the Fermi surface. The non-interacting Fermi surface is represented by a black line. The interacting Fermi surface is hole-like, centered at $(\pi, \pi)$, and encloses significantly more volume than the non-interacting Fermi surface. This indicates a violation of Luttinger's theorem.

An alternative way of mapping the Fermi surface, which also allows more direct contact with ARPES experiments, is to make constant energy plots of the single-particle spectra at the Fermi energy $A(\mathbf{k}, \omega = 0)$. The constant energy plots $A(\mathbf{k}, \omega = 0)$ are shown in Figs. 5, 6 and 7 for $n = 0.95$, $n = 0.90$ and $n = 0.80$, respectively, for the upper right quadrant of the first Brillouin zone. The regions of high density are colored in violet and low density in red. The solid black lines as before represent the non-interacting Fermi surface. For $n = 0.95$, the Fermi surface resulting from our calculations is hole-like, centered around $(\pi, \pi)$, and encloses a volume larger than the non-interacting Fermi surface, indicating a violation of Luttinger's theorem. In addition, the shape of the Fermi surface close to $(\pi/2, \pi/2)$, especially the clear shift above $(\pi/2, \pi/2)$ cannot be interpreted neither in terms of a simple tight-binding band structure nor a weak-coupling theory[29]. Note also that in comparison to the $|\nabla n(\mathbf{k})|$ result, no apparent electron like shadow band at $(\pi, 0)$ can be seen.

With increasing doping a bifurcation of the Fermi surface around $(\pi, 0)$ starts to develop (see Fig. 6), signalling the incipient crossover from a hole like Fermi surface to the expected electron like at large doping. In addition, around $(\pi/2, \pi/2)$ the peak in the spectrum follows more or less the noninteracting Fermi surface again. This points towards a restoration of Luttinger's theorem. For $n = 0.80$, the Fermi surface is definitely electron like, centered at $(0, 0)$, and has essentially the same volume and shape as the non-interacting surface, indicating a return to Fermi-liquid like behavior. No apparent remnants of the hole-like Fermi surface at lower doping are left. Interpreting these bifurcations seen most strongly around $n = 0.90$ as shadow Fermi surfaces, we find a strong reduction of the weight in these shadow features both for dopings less and larger than this "optimal" doping. Interestingly, a similar behavior was recently observed in the analysis of ARPES data for Bi2212[8]. However, in these experiments the Fermi surface remained hole-like throughout the whole doping regime studied. Whether this might be related to a finite $t'$ neglected in our present calculations will be discussed elsewhere.

### Summary and conclusions

The increasing precision and quality of experimental ARPES spectra in recent years has led to a number of new results on the single-particle dynamics of the high-$T_c$ cuprates, both partially resolving long-standing issues and posing new questions and problems. Motivated by especially the interesting observations concerning the changes of Fermi surface topology with doping, we have studied the two-dimensional (2D) Hubbard model with nearest neighbor hopping $t$ in the intermediate coupling regime (on-site correlation $U$ equal to the bandwidth) at

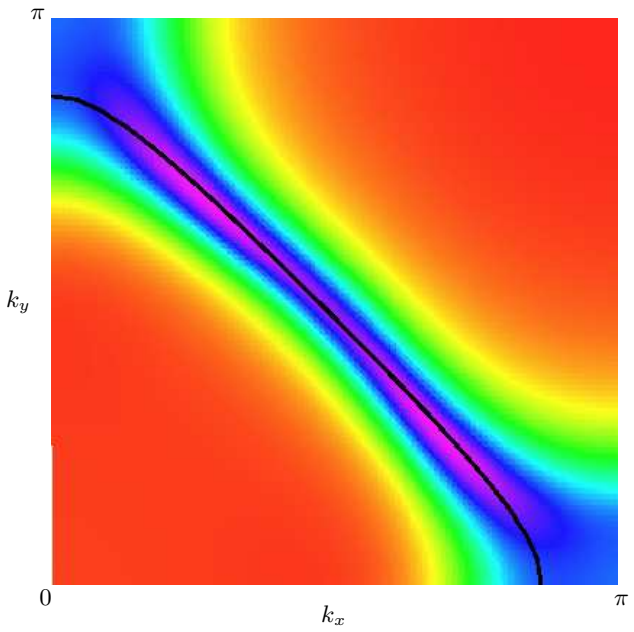


FIG. 6: Constant energy scans of $A(\mathbf{k}, \omega = 0)$ for $\delta = 0.1$, The other parameters and the color scheme are the same as in Fig. 5. The non-interacting and interacting Fermi surfaces start to coincide again, which can be interpreted as restoration of Luttinger's theorem. Note however the strong bifurcation around the $X$ point.

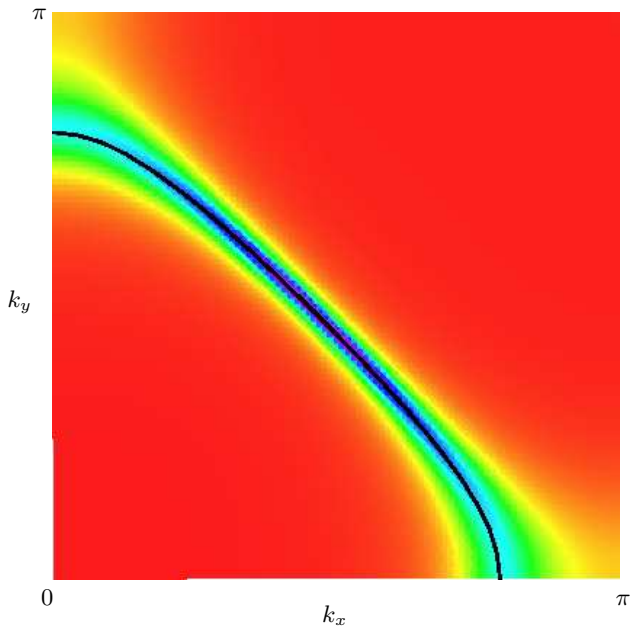


FIG. 7: Constant energy scans of $A(\mathbf{k}, \omega = 0)$ for $\delta = 0.2$. The other parameters and the color scheme are the same as in Fig. 5. The non-interacting and interacting Fermi surfaces coincide, in accord with Luttinger's theorem.

the temperature $T = 0.033$eV. To study the model in this most problematic parameter regime we used quantum Monte Carlo within the dynamical cluster approximation for the cluster size $N_c = 16$. Since this method allows for controlled and reliable calculations of low-energy features within a non-perturbative scheme and in the thermodynamic limit, fundamental problems in this field can be addressed. These include the single-particle spectral properties at low energies, especially possible deviations from Luttinger's theorem or the formation of non Fermi liquid states, and the resulting topology of the Fermi surface

¿From the two different ways to define the Fermi surface, i.e. via $|\nabla n(\vec{k})|$ and inspection of a constant energy scan $A(\vec{k}, \omega = 0)$ the latter turned out to be the more precise. The constant energy scans are able to distinguish the situation where a peak in the spectral crosses the Fermi surface from that where it only approaches it. Thus they were free of spurious bifurcations observed in the $|\nabla n(\vec{k})|$ plots. From the constant energy scans of the spectrum at the Fermi energy we find that the Fermi surface changes its topology compared to the non-interacting one as a function of decreasing doping. While the latter is closed around the zone center for every finite doping, the interacting Fermi surface at low doping, $\delta = 0.05$, is hole-like, closed around $M = (\pi, \pi)$. Moreover, the form and shifts present in the Fermi surface must be taken as clear evidence for a violation of Luttinger's theorem. Non Fermi liquid behavior is also evidenced by the spectrum. A strong particle-hole asymmetry is found at the Fermi surface crossing near $(\pi/2, \pi/2)$ with hole-like excitations having much longer life-times than electronic excitations. Furthermore the corresponding self-energy shows strong $\vec{k}$-dependence rendering local approximations like the DMFA irrelevant. Additional structures in the self energy and a rather large residual scattering rate can also be interpreted as signs for non Fermi liquid behavior. However, to really distinguish a non Fermi liquid from a Fermi liquid with a possibly extremely small energy scale much lower temperatures must be studied.

With increasing doping the Fermi surface bifurcates at $(\pi, 0)$ around a doping $\delta = 0.10$ and from the topology around $(\pi/2, \pi/2)$ one can infer a tendency towards restoration of Luttinger's theorem and conventional Fermi liquid behavior. Finally when $\delta = 0.20$ the Fermi surface is electron-like again, i.e. closed around the zone center, and coincides with the non-interacting Fermi surface. The corresponding spectra show well defined and sharp quasi-particle peaks around the Fermi energy with particle-hole symmetry being recovered in the low-energy region.

Although the Hubbard model surely presents an oversimplification of the real cuprates, the common belief is that at least the essential qualitative features of the low energy dynamics should be reproduced. In particular, the results presented here show some interesting qualitative agreement with experiments regarding the behavior

of the different structures observed in the spectra. Moreover, these features could be related to at least an apparent violation of Luttinger's theorem or possibly even non Fermi liquid behavior at low doping. From our results it becomes very clear that neither weak-coupling treatments nor local theories like the DMFT are able to capture the essentials of the physics of the cuprate in the weakly doped regime. There are, of course, a variety of further questions to be addressed. For example, most of the interesting and controversial ARPES results are for the system Bi2212, which actually is a bilayer system. Moreover, the simple nearest-neighbor tight binding band structure used in this paper is definitely not sufficient to describe the cuprates. Thus, a detailed study about the influence of a finite and negative $t'$ and also a bilayer coupling on the topology of the Fermi surface or more generally on the low-energy single particle dynamics is definitely necessary. We believe that such an investigation can also address some of the still mysterious features in behavior of the Fermi surface topology of the high-$T_c$ cuprates. Moreover it is very important to find new methods to solve the DCA self consistency cycle at lower temperatures or preferably at $T = 0$. This would enable us to clearly distinguish between a strong coupling Fermi liquid and genuine non Fermi liquid behavior at low doping.

### Acknowledgments

We acknowledge useful conversations with M. Hettler, C. Huscroft, H.R. Krishnamurthy, M. Sigrist, T.M. Rice. This work was supported by NSF grant DMR-0073308 and by the DFG Graduiertenkolleg "Komplexität in Festkörpern". We acknowledge supercomputer support by the Leibniz Rechenzentrum in Munich under grant h0301. This research was supported in part by NSF cooperative agreement ACI-9619020 through computing resources provided by the National Partnership for Advanced Computational Infrastructure at the Pittsburgh Supercomputer Center.

[1] For a review, see M.B. Maple, J. Mag. Mat. **177-181** pp18-30 (1998) ; J.L. Tallon and J.W. Loram, Physica C: Superconductivity **349**1-2 pp53-68 (2001).

[2] S.V. Borisenko, A.A. Kordyuk, S. Legner, C. Dürr, M. Knupfer, M.S. Golden, J. Fink, K. Nenkov, D. Eckert, G. Yang, S. Abell, H. Berger, L. Forró, B. Liang, A. Maljuk, C.T. Lin and B. Keimer, Phys. Rev. B**64**, 94513(2001).

[3] A. Damascelli, D.H. Lu and Z.-X. Shen, Journal of Electron Spectroscopy **117**–**118**, 165(2001).

[4] A. Kampf, J.R. Schrieffer, Phys. Rev. B**41**, 6399(1990); ibid **42**, 7967(1990); P. Aebi, J. Osterwalder, P. Schwaller, L. Schlapbach, M. Shimoda, T. Mochiku and K. Kadowaki, Phys. Rev. Lett. **72**, 2757(1994).

[5] For an overview see e.g. Ref. 3.

[6] A. Fujimori, A. Ino, T. Yoshida, T. Mizokawa, Z.-X. Shen, C. Kim, T. Kakeshita, H. Eisaki, S. Uchida in *Open Problems in Strongly Correlated Electron Systems*, J. Bonča, P. Prelovšek, A. Ramšak and S. Sakar (eds.), Kluwer Academic Publ. (2001), p. 119.

[7] T. Yoshida, X.J. Zhou, M. Nakamura, S.A. Kellar, P.V. Bogdanov, E.D. Lu, A. Lanzara, Z. Hussain, A. Ino, T. Mizokawa, A. Fujimori, H. Eisaki, C. Kim, Z.-X. Shen, T. Kakeshita and S. Uchida, Phys. Rev. B63, 220501(2001).

[8] A.A. Korduyk, S.V. Borisenko, M.S. Golden, S. Legner, K.A Nenkov, M. Knupfer and J. Fink, cond-mat/0104294.

[9] P.V. Bogdanov, A. Lanzara, X.J. Zhou, S.A. Kellar, D.L. Feng, E.D. Lu, H. Eisaki, J.-I. Shimoyama, K. Kishio, Z. Hussain and Z.X. Shen, cond-mat/0005394.

[10] Y.-D. Chuang, *et al.*, Phys. Rev. Lett. **83**, 3717 (1999); D.L. Feng *et al.*, unpublished, cond-mat/9908056.

[11] P.W. Anderson, **The Theory of Superconductivity in the High-$T_c$ Cuprates**, Princeton University Press, Princeton, NJ (1997).

[12] E. Dagotto, Reviews of Mod. Physics **66**, 763(1994).

[13] W.O. Putikka, M.U. Luchini and R.R.P. Singh, Phys. Rev. Letters **81**, 2966(1998).

[14] N. E. Bickers, D. J. Scalapino, S. R. White, Phys. Rev. Lett. **62**, 961 (1989).

[15] M.H. Hettler, A.N. Tahvildar-Zadeh, M. Jarrell, T. Pruschke and H. R. Krishnamurthy, Phys. Rev. B **58**, 7475 (1998); M.H. Hettler, M. Mukherjee, M. Jarrell and H. R. Krishnamurthy, Phys. Rev. B **61**, 12739 (2000).

[16] Th. Maier *et al.*, Eur. Phys. J. B **13**, 613 (2000); Th. Maier, M. Jarrell, Th. Pruschke, and J. Keller, Phys. Rev. Lett. **85**, 1524 (2000).

[17] C. Huscroft, M. Jarrell, Th. Maier, S. Moukouri, and A.N. Tahvildarzadeh, Phys. Rev. Lett. **86**, 139 (2001).

[18] S. Moukouri and M. Jarrell, to appear in Computer Simulations in Condensed Matter Physics VII, Eds. D.P. Landau, K. K. Mon, and H. B. Schuttler (Springer-Verlang, Heidelberg, Berlin, 2000).

[19] M. Jarrell, Th. Maier, C. Huscroft, S. Moukouri, Phys. Rev. B, to appear, cond-mat/0108140.

[20] T. Pruschke *et al.*, Adv. in Phys. **42**, 187 (1995); A. Georges *et al.*, Rev. Mod. Phys. **68**, 13 (1996).

[21] A.I. Lichtenstein and M.I. Katsnelson, Phys. Rev. B **62**, R9283 (2000).

[22] G. Kotliar, S.Y. Savrasov, G. Palsson, cond-mat/0010328.

[23] Th. Maier and M. Jarrell, to be publsihed.

[24] M. Jarrell, Phys. Rev. Lett. **69**, 168-71 (1992).

[25] R. Bulla, Th. Pruschke and A.C Hewson, J. Phys. – Condens. Matter **10**, 8365(1998).

[26] J.E. Hirsch and R.M. Fye, Phys. Rev. Lett. **56**, 2521 (1986).

[27] M. Jarrell and J.E. Gubernatis, Phys. Rep. **269**, 135 (1996).

[28] M.S. Hybertsen, E.B. Stechel, M. Schluter and D.R. Jennison, Phys. Rev. B41, 11068(1990); S.B. Bacci, E.R. Gagliano, R.M. Martin and J.F. Annett, Phys. Rev. B44, 7504(1991).

[29] V. Zlatić, B. Horvatić, B. Dolički, S. Grabowski, P. Entel, and K.-D. Schotte, Phys. Rev. B**63**, 35104(2001) and

references therein.
[30] S. Moukouri and M. Jarrell , unpublished.
[31] A. Ino, C. Kim, T. Mizokawa, Z.-X. Shen, A. Fujimori, M. Takaba, K. Tamasaku, H. Eisaki and S. Uchida, J. Phys. Soc. Jap. **68**, 1496(1999).
[32] J. Altmann, W. Brenig and A.P. Kampf, Eur. Phys. J. B**18**, 429(2000).